Optica Applicata, Vol. XLV, No. 1, 2015
DOI: 10.5277/oa150105

A method for improving the precision of on-line phase measurement profilometry

ZHUANG MAO, YIPING CAO*, LIJUN ZHONG, SENPENG CAO

Department of Optoelectronics, Sichuan University, Chengdu, China, 610064

*Corresponding author: ypcao@scu.edu.cn

An on-line phase measurement profilometry based on improved Stoilov's algorithm is proposed to measure the 3D shape of moving object. While only one frame sinusoidal grating is projected on the moving object, the equal phase-shifting step deformed patterns modulated by profile of the measured object can be captured at every equivalent moving distance of the measured object instead of digital phase-shifting. Stoilov's algorithm is an equal phase-shifting step algorithm at an arbitrary phase-shifting step, which is suitable for on-line phase measurement profilometry. However, the arbitrary phase-shifting step of Stoilov's algorithm depends on the captured deformed patterns, in which the digitized errors of digital light projector or CCD camera, and the disturbance of surrounding light could be introduced, it will lead to some abnormities in wrapped phase, such as the denominator in Stoilov's algorithm could be zero, which could cause the reconstructed 3D profile of the measured object appear burr, distortion or aberration, even could not be reconstructed. So an on-line phase measurement profilometry based on improved Stoilov's algorithm is proposed. The arbitrary phase-shifting step is retrieved by both pixel matching and fringe cycle calibration rather than the captured deformed patterns. Experiments verify the feasibility and effectiveness of the proposed on-line phase measurement profilometry.

Keywords: information optics, Stoilov's algorithm, phase measuring profilometry (PMP), on-line phase measurement profilometry (OPMP), phase-shifting, pixel matching.

1. Introduction

With the development of industrial automation, the application of industrial production line is getting more and more popular. In order to improve the efficiency of production line, and to make sure the high quality of products, the research of three-dimensional on-line measurement with high precision should be paid more and more attention. In the production line, the measured products are transported by the conveyor automatically to several appointed working procedures successively. One of the working procedures is the 3D shape measuring procedure. In this procedure, the measurement must be done on-line while the measured product is just being transported and the measured results must be of real-time to determine which working procedure should be appointed next. At present, phase measuring profilometry (PMP) [1–4] has the highest precision

in 3D profile measurement based on structured-light because its phase calculation is a point-to-point performance, but in traditional PMP, the measured object must remain static and N steps ($N > 2$) of phase-shifting must be needed and each phase-shifting step must be equivalent and be $2\pi/N$ strictly. It is difficult to meet the above requirement due to the movement of the measured object, which means the traditional PMP is not suitable for on-line measurement. Stoilov's algorithm [5] is an equal phase-shifting step algorithm at an arbitrary phase-shifting step, in other words, the sum of phase-shifting step does not need to be the integer multiple of 2π. The quantity of phase-shifting steps is not necessarily controlled strictly in Stoilov's algorithm, so the equivalent phase-shifting step can be obtained by the movement of the measured object, which is suitable for an on-line phase measurement profilometry (OPMP) [6–9]. However, the phase computing of Stoilov's algorithm depends on the captured deformed patterns, so the errors of a digital light projector (DLP) or CCD camera, and the disturbance of surrounding light could lead to some abnormities in a wrapped phase, which could cause the reconstructed 3D profile of the measured object appears blurred, distorted or aberrant, and even could not be reconstructed [10, 11]. Therefore, WU YING-CHUN *et al.* [12] proposed an active phase-shifting step OPMP method which an auxiliary positioning device to actively control the phase-shifting step. This method can be applied in some specific production lines with positioning device themselves. But most production lines have no positioning device. The universality of this method faces the challenge. So, a new OPMP based on improved Stoilov's algorithm is proposed which does not need any auxiliary device and is suitable for almost any production line with straight-line movement.

2. Principle

In traditional PMP, the measured object should remain static. While a group of phase-shifting sinusoidal gratings are projected on the measured object separately, the corresponding deformed patterns are captured and phase distribution can be calculated from these deformed patterns. After phase unwrapping and phase-to-height mapping [13–15], the 3D profile of the measured object can be reconstructed. In OPMP, the measured object is moving. In Fig. 1, the projection on the measured object is obtained by a parallel light irradiating a fixed sinusoidal grating. A CCD is used to capture N frames deformed patterns when the object has been moved through every equivalent moving distance S. The captured deformed patterns $I_i(x_i, y_i)$ can be described as follows:

$$I_i(x_i, y_i) = R(x_i, y_i)\left\{A(x_i, y_i) + B(x_i, y_i)\cos\left[\Phi(x_i, y_i) + i\Delta\right]\right\}, \quad i = 0, 1, 2, \ldots \tag{1}$$

where x_i and y_i represent the coordinate of a camera coordinate, $R(x_i, y_i)$ is the object's surface reflectivity, $A(x_i, y_i)$ is the ambient light, $B(x_i, y_i)/A(x_i, y_i)$ is the fringe contrast, $\Phi(x_i, y_j)$ is the phase of the deformed fringe patterns modulated by the height of the object, Δ is the equivalent phase-shifting step, which is less than 2π.

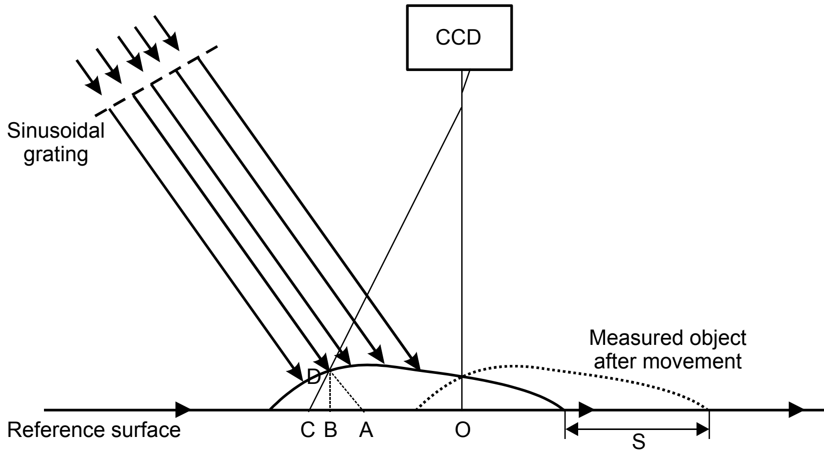

Fig. 1. PMP principle figure for on-line measurement.

When the measured object is moved, the coordinates of this measured object in different deformed patterns will be changed, so the $R(x_i,\ y_i)$ and $\Phi(x_i,\ y_j)$ in different captured deformed patterns are different. In order to calculate phase distribution, pixel matching [16–19] must be carried out to guarantee that equivalent deformed patterns (in which the coordinates of the measured object remain the same) can be extracted.

The pixel matching of the image frame 2–5 can be denoted as:

$$I_i'(x_0, y_0) = \Pi\{I_i(x_i, y_i), I_0'(x_0, y_0)\}, \qquad i = 0, 1, 2, 3, 4 \tag{2}$$

where $I_1'(x_0, y_0)$ is the equivalent deformed pattern extracted from the image frame 2 and frame 1 in Fig. 2, Π is the pixel matching operator, which means that pixel matching is carried out on the captured deformed pattern $I_i(x_i, y_i)$ and $I_0'(x_0, y_0)$ to get equivalent deformed patterns $I_i'(x_0, y_0)$.

The distribution of phase should be obtained by the following equation with Stoilov's algorithm:

$$\begin{cases} \Phi'(x_0, y_0) = \operatorname{atan}\left\{\dfrac{2[I_1'(x_0, y_0) - I_4'(x_0, y_0)]}{2I_2'(x_0, y_0) - I_0'(x_0, y_0) - I_4'(x_0, y_0)}\sin(\Delta)\right\} \\ \sin(\Delta) = \sqrt{1 - \left\{\dfrac{I_0'(x_0, y_0) - I_4'(x_0, y_0)}{2[I_1'(x_0, y_0) - I_3'(x_0, y_0)]}\right\}^2} \end{cases} \tag{3}$$

where $\Phi'(x_0, y_0)$ is a wrapped phase which is restricted between $-\pi$ to π, so phase unwrapping is used to get the continuous phase $\Psi'(x_0, y_0)$, and after phase-to-height mapping, the 3D profile of the measured object $H(x_0, y_0)$ can be reconstructed.

However, the second formula in Eq. (3) shows that the equivalent phase-shifting step Δ depends on the equivalent deformed patterns $I_i'(x_0, y_0)$, which are extracted

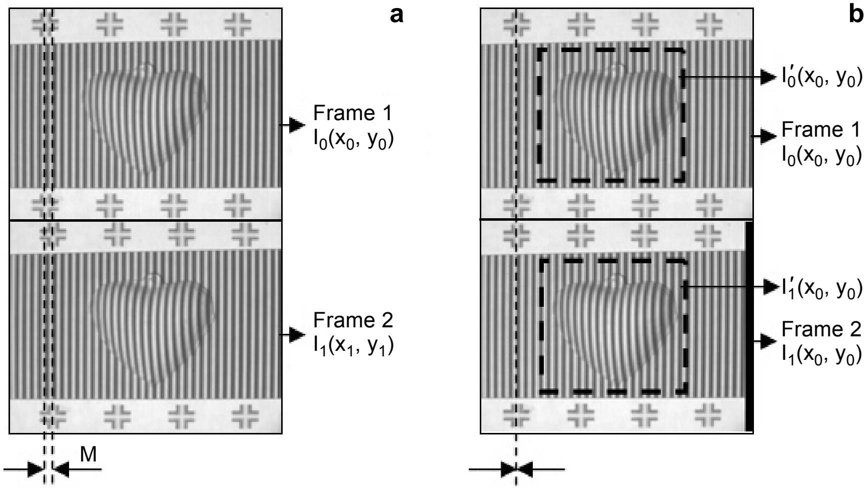

Fig. 2. Before (**a**) and after (**b**) pixel matching.

from the captured deformed patterns $I_i(x_i, y_i)$. Unfortunately, the digitized errors of a DLP or CCD camera, and the disturbance of surrounding light could let the $I'_i(x_0, y_0)$ contain errors, which could cause some unexpected abnormities in Δ calculation.

Firstly, because $I'_1(x_0, y_0)$ and $I'_3(x_0, y_0)$ contain errors, it is possible to meet the condition of $I'_1(x_0, y_0) = I'_3(x_0, y_0)$ somewhere, which will result in the fact that the denominator is to be zero, so as to make Δ meaningless. And the reconstructed 3D profile of the measured object contains a regional fracture at these places where phase computing is unrealizable, which means that the 3D profile of the measured object could not be reconstructed in this situation.

Secondly, because all of $I'_i(x_0, y_0)$ ($i = 0, 1, 2, 3, 4$) contain errors, it is also possible to meet the condition of $\left\{ \dfrac{I'_0(x_0, y_0) - I'_4(x_0, y_0)}{2[I'_1(x_0, y_0) - I'_3(x_0, y_0)]} \right\}^2 > 1$ somewhere, which will make Δ be a complex, so as to make Δ not consistent with its real number feature, which means the 3D profile of the measured object could not be reconstructed in this situation.

Additionally, Δ in Stoilov's algorithm is arbitrary and space-invariant. When Δ is not 90°, the errors in $I'_1(x_0, y_0)$ and $I'_3(x_0, y_0)$ would meet the condition of $I'_1(x_0, y_0) = I'_3(x_0, y_0)$ somewhere to compel Δ to be 90°, so the phase computing errors will be introduced, which means the reconstructed 3D profile of the measured object will contain blur, distortion or aberration.

Therefore, an OPMP based on the improved Stoilov's algorithm is proposed.

3. Improvement of Stoilov's algorithm

As discussed above, the original Stoilov's algorithm possibly contains some abnormities because of its dependence on the captured deformed patterns. With the analysis

of the equivalent phase-shifting step Δ in OPMP, it is found that Δ is controlled by the moving distance S of the measured object. If the fringe cycle L on the reference surface is known, Δ can be obtained in the world coordinate as:

$$\Delta = \frac{S}{L}2\pi \tag{4}$$

If the system calibration can be done to obtain the world coordinate to the pixel coordinate mapping K, Δ can also be denoted in the pixel coordinate as:

$$\Delta = \frac{S/K}{L/K}2\pi = \frac{M}{T}2\pi \tag{5}$$

where T is the fringe pixel cycle of the captured sinusoidal grating on the reference surface, M is the pixel difference between every adjacent captured deformed pattern that can be obtained by pixel matching as shown in Fig. 2; it can be corrected to the subpixel level. But the phase computing in Eq. (3) can be only achieved at every integer pixel, so the non-integer of M will lead to an additional shifting phase error. Therefore, M calibration to ensure M approximate to an integer, and T calibration are the keys to obtain a Δ with high precision.

3.1. *M* calibration

As discussed above, if the Δ is calculated in pixel coordinate, the K must be obtained in advance by system calibration. In order to get a K with high precision, making the most of the CCD camera field of view is very important. As shown in Fig. 3, a group of particular symmetric marks are designed to be pasted on the reference surface of the on-line bench and made a line just particular to the X moving direction of the on-line bench, so that the centroid of the interested mark captured by CCD can be extracted quickly and accurately by image processing. The system calibration steps are as follows.

Firstly, the on-line bench is precisely controlled to make the interested mark Q on the reference surface locate at the left edge of the CCD camera field of view as close

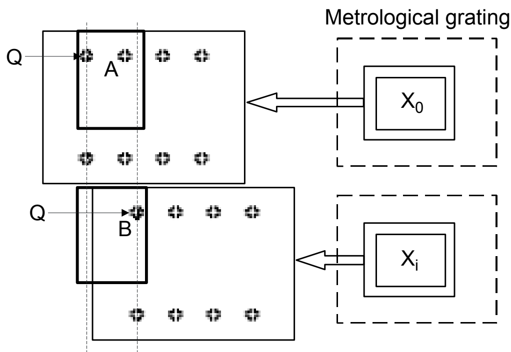

Fig. 3. System calibration of reference plane.

as possible and the position X_0 of the on-line bench is recorded by a metrological grating while capturing the image frame A. Secondly, the on-line bench is precisely controlled to make the corresponding interested mark Q on the reference surface locate at the right edge of the CCD camera field of view as close as possible and the position X_i of the on-line bench is recorded by the metrological grating while capturing the image frame B. Lastly, by image processing, the centroids of Q along the X direction C_0 in the image frame A and C_i in the image frame B can be extracted precisely. Then, the world coordinate to the pixel coordinate mapping K can be calibrated as

$$K = \frac{X_i - X_0}{C_i - C_0} \tag{6}$$

In OPMP, as shown in Fig. 3, the strict control over the moving distance S must be carried out to improve the additional shifting phase errors as discussed above. The diagram of M calibration is shown in Fig. 4.

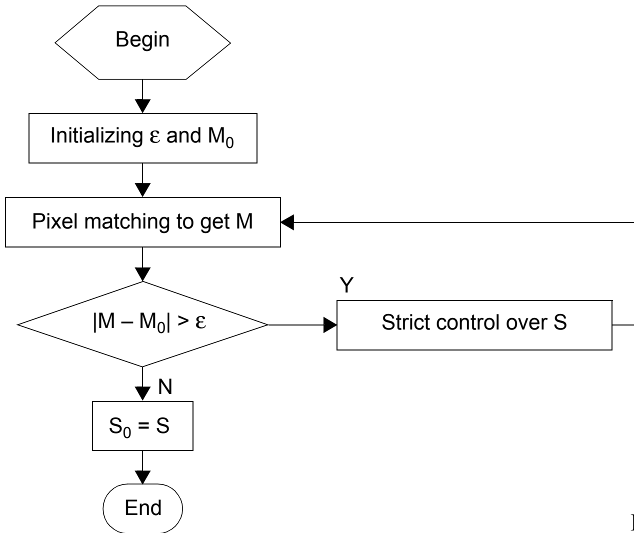

Fig. 4. Diagram of M calibration.

A suitable infinitesimal $\varepsilon > 0$ is used as the ending condition of M calibration and the expected M is initialized as an integer M_0 at the beginning of M calibration. By strict control over S repeatedly until M approximate to M_0 as closer as expected, then the S at this condition is recorded as S_0. In this way, the pixel difference caused by S_0 will be a good fit to the integer M_0.

If the S_0 is converted into the pulse number N_0 of the metrological grating and is preset in the transmitter circuit on the metrological grating electrical control device. While the on-line bench is moving along the X direction, the transmitter circuit can automatically trigger the CCD camera to capture deformed patterns at intervals of

a certain S_0 to make sure every two adjacent captured deformed patterns have an equal shifting phase with high precision, and the speed of the measured object may be nonuniform as long as the CCD camera can capture clear deformed patterns during the measurement.

3.2. *T* calibration

Indeed, the fringe pixel cycle T on the reference surface could be obtained by image processing directly. However, the precision of T is somehow limited in this way, so a new method based on PMP is proposed, in which the T can be calibrated by computing the wrapped phase of a captured sinusoidal grating on the reference surface. While five sinusoidal grating patterns with an interval shifting phase of 2π/5 are projected on the reference surface respectively, the five corresponding phase-shifting fringe images $I_j^0(x, y)$ $(j = 0, 1, 2, 3, 4)$ can be captured by a CCD camera, and the wrapped phase Phase(x, y) of the reference surface can be obtained:

$$\text{Phase}(x, y) = \text{atan}\left[\frac{\sum_{j=0}^{4} I_j^0(x, y)\sin(2\pi j/5)}{\sum_{j=0}^{4} I_j^0(x, y)\cos(2\pi j/5)}\right], \quad j = 0, 1, 2, 3, 4 \tag{7}$$

Because the fringes are projected on the reference surface, the profile of the wrapped phase shows a sawtooth wave as shown in Fig. 5**a**. It is well-known that T is well reflected by the cycle P of the sawtooth wave. If there are not any errors caused by the CCD camera and DLP, the pixel difference along the X direction between any two adjacent identical phase points in the wrapped phase can denote P. Unfortunately, the errors caused by the CCD camera and DLP are non-ignorable, so a mean-approaching algorithm of P is applied to restrain the errors efficiently.

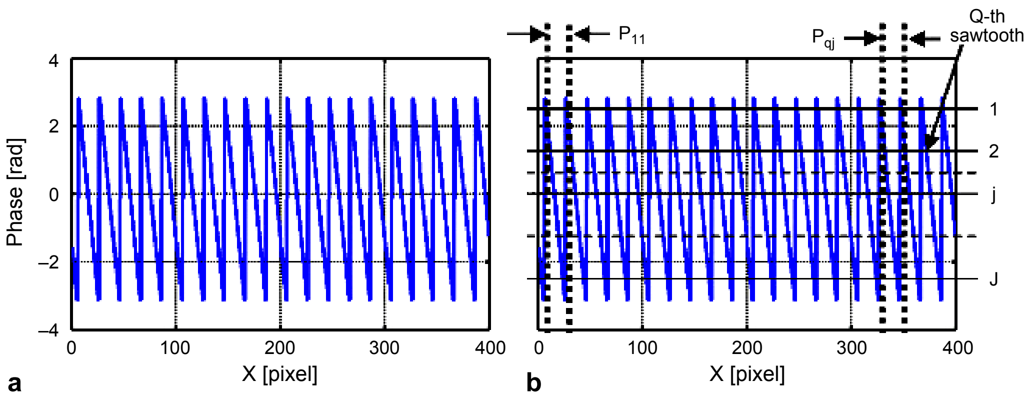

Fig. 5. The profile of wrapped phased (**a**) and its cycle approaching (**b**).

As shown in Fig. 5**b**, J identical phase lines are drawn on the sawtooth wave and there are Q sawteeth along the X direction. P_{qj} is denoted as the pixel difference between the q-th intersection and the $(q + 1)$-th intersection across the j-th identical phase line, and P_j is the average pixel difference of all the intersections across the j-th identical phase line

$$P_j = \frac{\sum_{q=1}^{Q-1} P_{qj}}{Q-1} \tag{8}$$

Then, the P can be denoted as

$$P \approx \overline{P} = \frac{\sum_{j=1}^{J} P_j}{J} \tag{9}$$

So, the calibrated T can be reflected by P and is denoted by T_0

$$T_0 = P \tag{10}$$

3.3. The improved PMP algorithm

With the calibration of T and strict control over S, the equivalent phase-shifting step Δ_0 can be obtained and the improved Stoilov's algorithm can be expressed as

$$\begin{cases} \Phi'(x_0, y_0) = \operatorname{atan}\left\{ \dfrac{2[I'_1(x_0, y_0) - I'_4(x_0, y_0)]}{2I'_2(x_0, y_0) - I'_0(x_0, y_0) - I'_4(x_0, y_0)} \sin(\Delta_0) \right\} \\ \Delta_0 = \dfrac{M_0}{T_0} \end{cases} \tag{11}$$

The digitized errors of DLP or CCD camera, the non-linear errors and the disturbance of surrounding light can be reduced to some extend.

4. Experimental results and analysis

In order to verify the feasibility and validity of the proposed OPMP based on improved Stoilov's algorithm, a series of experiments were carried out. The experimental system is shown in Fig. 6, in which the model of DLP is CP-H6500, the model of CCD in this system is MTV1881EX, whose frame rate is 60 frame/s, exposure time can range from 1/50 s to 1/10000 s, and 1/500 s is selected. Figure 7 shows the comparative result of 3D profile of the measured object by the original Stoilov's algorithm and the improved Stoilov's algorithm. The 3D profile of the measured object reconstructed by the original Stoilov's algorithm in Fig. 7**a** has a blur, and its surface shows a regional fracture.

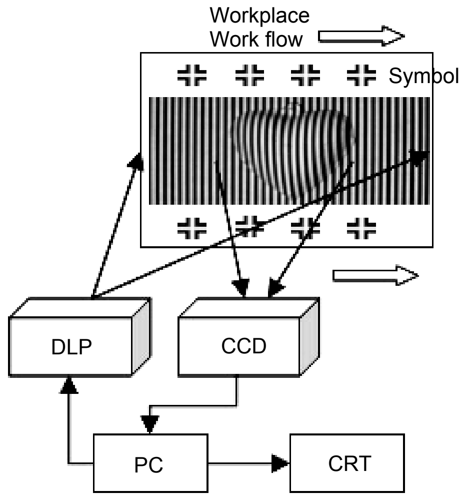

Fig. 6. Experiment system.

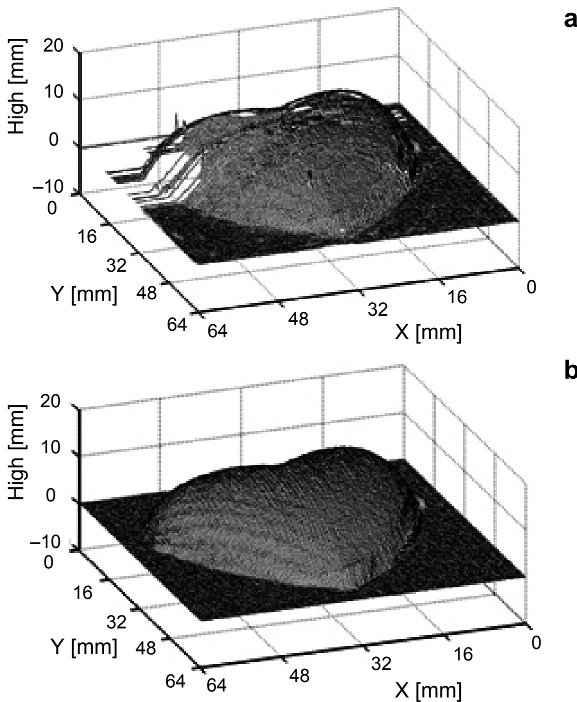

Fig. 7. Reconstructed object by original (**a**) and improved (**b**) algorithm.

Some local profiles cannot be reconstructed because of some unexpected abnormalities in Δ calculation. In Fig. 7**b**, the 3D profile of the measured object has been reconstructed completely by the improved Stoilov's algorithm and remains smooth and realistic, which verifies the feasibility and validity of the proposed OPMP.

5. Conclusion

An experimental system suitable for OPMP is established, and in OPMP based on the original Stoilov's algorithm, the equivalent phase-shifting step depends on the equivalent deformed patterns, which are extracted from captured deformed patterns. Unfortunately, the digitized errors of a DLP or CCD camera, and the disturbance of surrounding light could cause some unexpected abnormalities in the equivalent phase calculation. Then, a solution based on pixel matching and fringe cycle calibration is proposed. With the proposed OPMP, based on the improved Stoilov's algorithm, the experiment results show that there is not any abnormity in the equivalent phase calculation, and the reconstructed 3D profile of a moving object is smooth and realistic. The validity and feasibility of the proposed OPMP are verified by a series of experiments and the accuracy of 3D on-line measurement has been improved effectively.

Acknowledgements – This work was supported by the 863 National Plan Foundation of China under Grant No. 2007AA01Z333 and Special Grand National Project of China under grant No. 2009ZX02204-008.

References

[1] QINGYANG WU, XIANYU SU, LIQUN XIANG, YUBAO LI, *A new calibration method for two-sensor measurement system based on line-structure light*, Chinese Journal of Lasers **34**(2), 2007, pp. 259–264.
[2] CHEN F., BROWN G.M., SONG M., *Overview of three-dimensional shape measurement using optical methods*, Optical Engineering **39**(1), 2000, pp. 10–22.
[3] YONEYAMA S., MORIMOTO Y., FUJIGAKI M., YABE M., *Phase-measuring profilometry of moving object without phase-shifting device*, Optics and Lasers in Engineering **40**(3), 2003, pp. 153–161.
[4] YONGJIAN ZHU, ANHU LI, WEIQING PAN, *Discussions on phase-reconstruction algorithms for 3D digitizing structure-light profilometry*, Optik – International Journal for Light and Electron Optics **122**(2), 2011, pp. 162–167.
[5] STOILOV G., DRAGOSTINOV T., *Phase-stepping interferometry: five-frame algorithm with an arbitrary step*, Optics and Lasers in Engineering **28**(1), 1997, pp. 61–69.
[6] WU YINGCHUN, CAO YIPING, LU MINGTENG, LI KUN, *An on-line phase measuring profilometry based on modulation*, Optica Applicata **42**(1), 2012, pp. 31–41.
[7] JIAHUI PAN, PEISHEN S. HUANG, FU-PEN CHIANG, *Color phase-shifting technique for three-dimensional shape measurement*, Optical Engineering **45**(1), 2006, article 013602.
[8] BERRYMAN F., PYNSENT P., CUBILLO J., *A theoretical comparison of three fringe analysis methods for determining the three-dimensional shape of an object in the presence of noise*, Optics and Lasers in Engineering **39**(1), 2003, pp. 35–30.
[9] FARRELL C.T., PLAYER M.A., *Phase step measurement and variable step algorithms in phase-shifting interferometry*, Measurement Science and Technology **3**(10), 1992, pp. 953–958.
[10] BROPHY C.P., *Effect of intensity error correlation on the computed phase of phase-shifting interfereometry*, Journal of the Optical Society of America A **7**(4), 1990, pp. 537–541.
[11] LIAN XUE, XIANYU SU, *Phase-unwrapping algorithm based on frequency analysis for measurement of a complex object by the phase-measuring-profilometry method*, Applied Optics **40**(8), 2001, pp. 1207–1215.
[12] WU YING-CHUN, CAO YI-PING, ZHONG LI-JUN, *An improved method of stoilov algorithm adapting to phase measuring profilometry*, Acta Photonica Sinica **39**(2), 2010, pp. 307–310.
[13] WENSHEN ZHOU, XIANYU SU, *A direct mapping algorithm for phase-measuring profilometry*, Journal of Modern Optics **41**(1), 1994, pp. 89–94.

[14] WANSONG LI, XIANYU SU, ZHONGBAO LIU, *Large-scale three-dimensional object measurement: a practical coordinate mapping and image data-patching method*, Applied Optics **40**(20), 2001, pp. 3326–3333.

[15] YUANYUAN CAI, XIANYU SU, *Inverse projected-fringe technique based on multi projectors*, Optics and Lasers in Engineering **45**(10), 2007, pp. 1028–1034.

[16] KEYSERS D., DESELAERS T., NEY H., *Pixel-to-pixel matching for image recognition using Hungarian graph matching*, Pattern Recognition, Lecture Notes in Computer Science, Vol. 3175, 2004, pp. 154–162.

[17] CHARAN R., AHUJA N., *Feature guided pixel matching and segmentation in motion image sequences*, IEEE Proceedings of International Symposium on Computer Vision, 1995, pp. 277–282.

[18] KUANG PENG, YI-PING CAO, KUN LI, YING-CHUN WU, *A new pixel matching method using the entire modulation of the measured object in online PMP*, Optik – International Journal for Light and Electron Optics **125**(1), 2014, pp. 137–140.

[19] KO-CHEUNG HUI,WAN-CHI SIU,YUI-LAM CHAN, *New adaptive partial distortion search using clustered pixel matching error characteristic*, IEEE Transactions on Image Processing **14**(5), 2005, pp. 597–607.

Received August 25, 2014
in revised form November 24, 2014